International Journal of ChemTech Research
CODEN (USA): IJCRGG, ISSN: 0974-4290, ISSN(Online):2455-9555
Vol.10 No.5, pp 0994-1013, 2017

Passive Lossless Clamped Converter for Hybrid Electric Vehicle

R.Samuel Rajesh Babu, D.Jamuna Rani, K.P Indira, Kamesh.J, Kameshvar.S

Department of Electronics & Instrumentation Engineering, Faculty of Electrical & Electronics Engineering, Sathyabama University, Chennai, India.

Abstract : This paper presents a comparative analysis of Passive Lossless Clamped (PLC) Converter for Hybrid Electric Vehicle using Renewable Energy. The proposed converter is devised for boosting the voltage generated from the fuel cell through three winding coupled output inductor and voltage doublers circuit. The proposed converter achieves high step-up voltage gain without large duty cycle. The passive lossless clamped technology not only recycles leakage energy to improve efficiency but also alleviates large voltage spike to limit the voltage stress. The proposed converter is simulated in open and closed loop using PID and FUZZY controller. The simulation results are verified experimentally and the output of the proposed converter is free from ripples and has regulated output voltage.
Keywords : Passive Lossless Clamped (PLC) Converter, Three winding coupled output inductor, High step-up voltage gain, Fuzzy controller, Hybrid electric vehicle.

Introduction

Recently, the cost increase of fossil fuel and new regulations of Co_2 emissions have strongly increased the interests in renewable energy sources[1,2,3,5–9]. Hence, renewable energy sources such as fuel cells, solar energy and wind power have been widely valued and employed. Fuel cells have been considered as an excellent candidate to replace the conventional diesel or gasoline in vehicles and emergency power sources. Fuel cells can provide clean energy to users without Co_2 emissions. Due to stable operation with high-efficiency and sustainable or renewable fuel supply, fuel cell has been increasingly accepted as a competently alternative source for the future.

The excellent features of fuel cell are small size and high conversion efficiency makes them valuable and potential[10,11,12,13,15–19]. Hence, the fuel cell is suitable for power supplies in Renewable energy source applications. In typical fuel cell power supply system containing a high step-up converter, the generated voltage of the fuel cell stack is rather low. Hence, a high step-up converter is strongly required to lift the voltage for applications such as DC microgrid, inverter and battery. Ideally, a conventional boost converter is able to achieve high step-up voltage gain with an extreme duty cycle. The step-up voltage gain is limited by effects of the power switch, rectifier diode and the resistances of the inductors and capacitors. In addition, the extreme duty cycle may result in a serious reverse-recovery problem and conduction losses. A flyback converter is able to achieve high step-up voltage gain by adjusting the turns ratio of the transformer winding. However, a large voltage spike leakage energy causes may destroy the main switch. In order to protect the switching devices and constrain the voltage spike, a high-voltage-rated switch with high on-state resistance (*R*DS-ON) and a snubber circuit are usually adopted in the flyback converter, but the leakage energy still be consumed. These methods will diminish the power conversion efficiency.

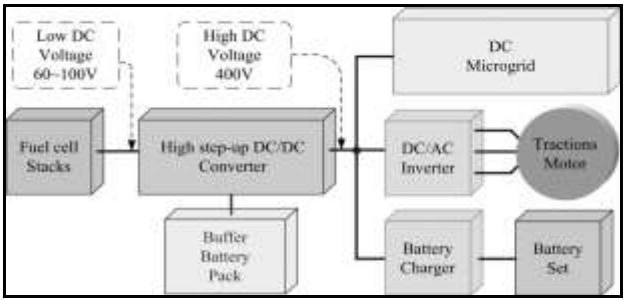

Figure 1.1 Fuel cell power supply system with high step-up converter.

In order to increase the conversion efficiency and voltage gain, many technologies such as zero-voltage switching (ZVS), zero-current switching (ZCS), coupled inductor and active clamp have been investigated. Some high step-up voltage gain can be achieved by using switched-capacitor and voltage-lift techniques, although switches will suffer high current and conduction losses.

In conventional circuit, the converter results in low voltage gain, low efficiency and high voltage stress. To overcome these problems Passive Lossless Clamped (PLC) Converter with three winding coupled output inductor has been proposed [20,21,22,23,24–25].

2. Operating Principle of Passive Lossless Clamped (PLC) Converter With Three-Winding Coupled Inductor

The proposed converter employs a switched capacitor and a Voltage-Doubler circuit for high step-up conversion ratio. The switched capacitor supplies an extra step-up performance, the Voltage-Doubler circuit lifts of the output voltage by increasing the turn's ratio of coupled-inductor. The advantages of proposed converter are as follows

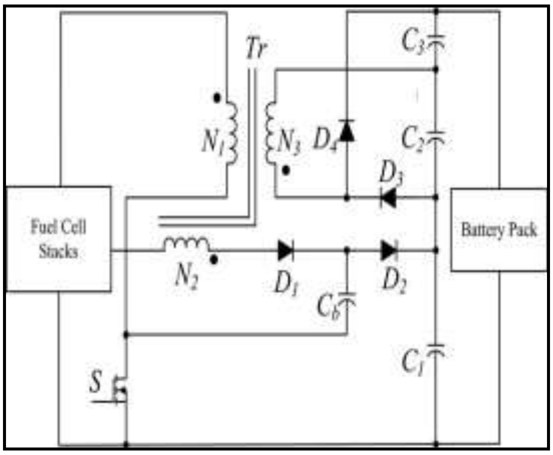

Figure 2.1 Passive Lossless Clamped (PLC) Converter

1. By adjusting the turns ratio of coupled inductor, the proposed converter achieves high step-up gain for the renewable energy systems.
2. The leakage energy is recycled to the output terminal, which improves the efficiency and alleviates large voltage spikes across the main switch.
3. Due to the passive lossless clamped performance, the voltage stress across main switch is substantially lower than the output voltage.
4. Low cost and high efficiency are achieved by adopting low-voltage-rated power switch with low *R*DS-ON.
5. By using three-winding coupled inductor, the proposed converter achieves more flexible adjustment of voltage conversion ratio and voltage stress on each diode.

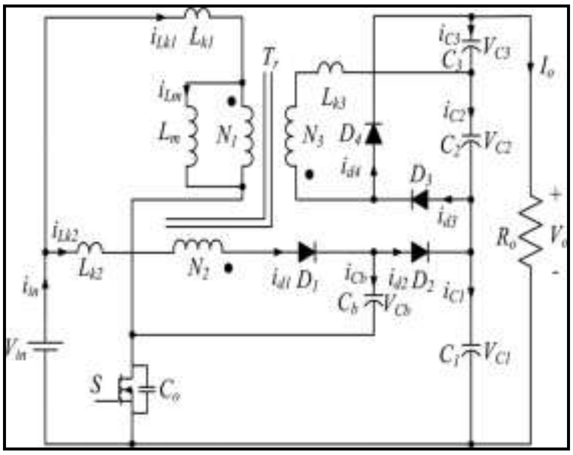

Figure.2.2 Equivalent circuit of Passive Lossless Clamped (PLC) Converter with three-winding coupled inductor

The equivalent circuit of the proposed converter is composed of a coupled inductor T_r, a main power switch S, diodes D_1, D_2, D_3, and D_4 , the switched capacitor C_b , and the output filter capacitors C_1, C_2 and C_3 . Lm is the magnetizing inductor and L_{k1}, L_{k2} and L_{k3} represent the leakage inductors. The turns ratio of coupled inductor n_2 is equal to N_2/N_1 and n_3 is equal to N_3/N_1 where N_1,N_2 and N_3 are the winding turns of the coupled inductor.

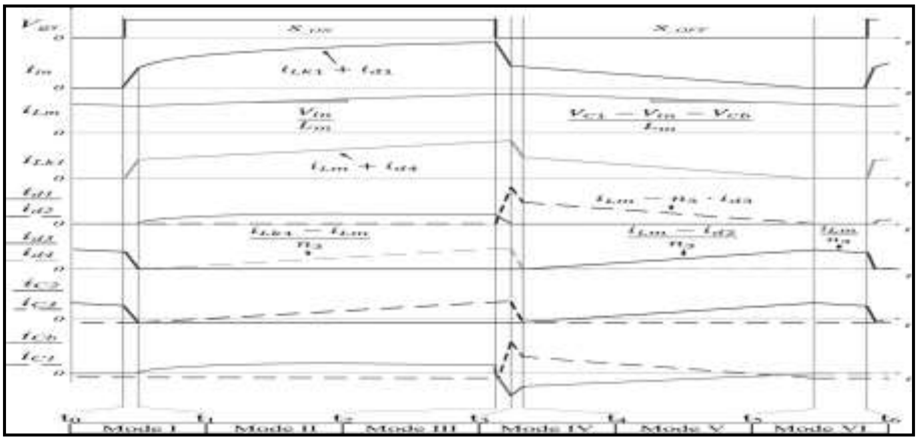

Figure.2.3 Steady-state waveforms in CCM operation.

2.1. Modes of Operation

Mode I [t_0, t_1]: During this interval, the switch S is turned ON at t_0. The diodes D_1,D_2 and D_4 are reverse biased. The path of current flow is shown in FIGURE. 2.5(a). The primary leakage inductor current iL_{k1} increases linearly and the energy stored in magnetizing inductance is transferred to the load and output capacitor C_2 via diode D_3.

Mode II [t_1, t_2]: During this interval, the switch S is in the turn-on state. The diodes D_1 and D_4 are forward biased, diodes D_2 andD_3 are reverse biased. The path of current flow is shown in FIGURE. 2.5(b). The DC source V_{in} still charges into the magnetizing inductor L_m and leakage inductor L_{k1} and the currents through these inductors rise linearly. Some of the energy from DC source V_{in} transfer to the secondary side of the coupled inductor to charge the capacitor C_3. The switched capacitor C_b is charged by the LC series circuit.

Mode III [t_2, t_3]: During this interval, the switch S is turned OFF at t_2 .DiodesD_1 andD_4 are forward biased, diodesD_2 and D_3 are reverse biased. The path of current flow is shown in FIGURE. 2.5(c). The magnetizing current and LC series current charge the parasitic capacitor C_o of the MOSFET.

Mode IV [t_3, t_4]: During this interval, the switch S is in the turnoff state. The diodes D_1,D_2 and D_4 are forward biased. The diode D_3 is reverse biased. The current-flow path is shown in FIGURE. 2.5(d). The current id_4 charges the output capacitor C_3 and decreases linearly. The total voltage of V_{in}+ VL_m+ VC_b is charging to clamped capacitor C_1 and some of the energy is supplied to the load.

Mode V [t_4, t_5]: During this interval, switch S is in the turn-off state. The diodes D_1 and D_4 are turned OFF, the diodes D_2 and D_3 are forward biased. The current-flow path is shown in FIGURE. 2.5(e). The energy of the primary side still charges to the clamped capacitor C_1 and supplies energy to the load. Some of the energy from DC source V_{in} is transferred to the secondary side of the coupled inductor to charge the capacitor C_2 and the current id_3 increases linearly.

Mode VI [t_5, t_6]: During this interval, switch S is in the turn-off state. The diodesD_1,D_2 and D_4 are reverse biased and the diode D_3 is forward biased. The current-flow path is shown in FIGURE. 2.5(f). The current iLk_1 is dropped till zero. The magnetizing inductor L_m continuously transfers energy to the third leakage inductor Lk_3 and the capacitor C_2 . The energies are discharged from C_1 and C_3 to the load. The current id_3 charges C_2 and supplies the load current.

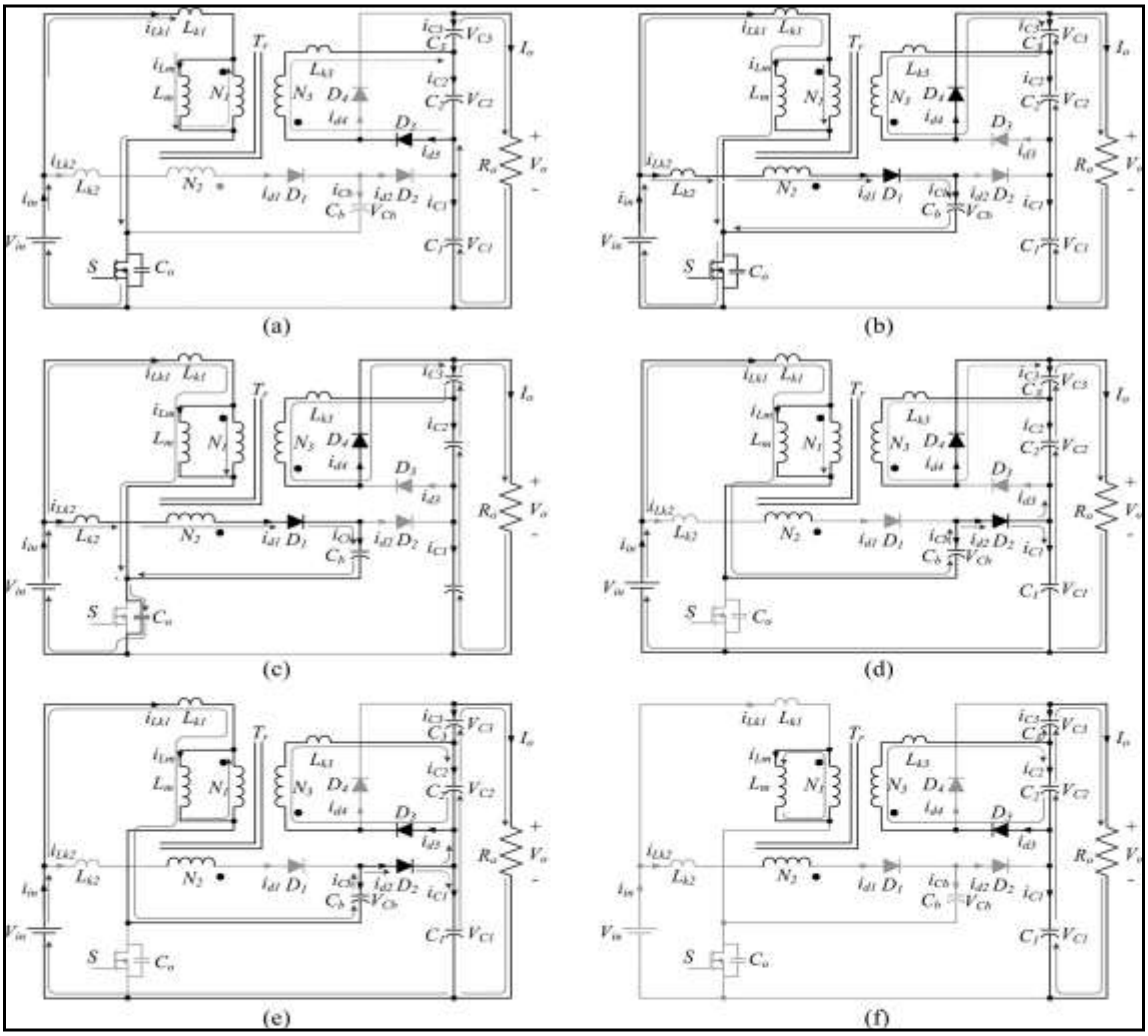

Figure.2.4 CCM operating modes of the PLC converter. (a) Mode I [t_0 , t_1]. (b)Mode II [t_1 , t_2]. (c)Mode III [t_2 , t_3]. (d)Mode IV [t_3 , t_4]. (e)Mode V [t_4 ,t_5].(f) Mode VI [t_5 , t_6].

3. Steady-State Analysis

In CCM steady-state analysis, the following factors are taken into account. In Passive Lossless Clamped (PLC) Converter with three-winding coupled output inductor all the leakage inductors of the coupled inductor are neglected and all components are ideal without any parasitic components. The voltages V_b , V_{C1} ,

V_{C2} and V_{C3} are considered to be constant due to infinitely large capacitances.

A. Step-Up Gain

During the turn-on period of switch *S*, the following equations can be written as

$V_{C3}=V_{N3}=n_3.Vin$ (1)
$V_{CB}=V_{IN}+V_{N2}=(N_2+1).V_{IN}$ (2)

During the turn-off period of switch *S*, the following equations can be expressed as:

$V_{C2}= n_3[V_{C1}-(2+n_2).V_{IN}$ (3)
$V_{C1}=(\frac{D}{1-D}+2+n_2).V_{in}$ (4)

Thus, the output voltage V_O can be expressed as

$V_O=V_{C1}+V_{C2}+V_{C3}$ (5)

By substituting (1), (3) and (4) into (5), the voltage gain of the proposed converter is given by

$M_{CCM} =\frac{Vo}{Vin}=n_2+\frac{2-D+N3}{1-D}$ (6)

Equation (6) shows that high step-up gain can be easily obtained by increasing the turns ratio of the coupled inductor without large duty cycle.

B.Voltage Stress

When the switching *S* is turned OFF, the diodes D_1 and D_3 are reverse biased. Therefore, the voltage stresses of D_1 and D_3 are as follows:

$M_{D1}= \frac{VD1}{VOUT}=\frac{1+N2}{2-D+(1-D)N2+N3}$ (8)

$M_{D4}= \frac{VD3}{VOUT}=\frac{1}{2-D+(1-D)N2+N3}$ (9)

When the switch *S* is in turn-on period and the diodes D_2 and D_3 are reverse biased. Therefore, the voltage stresses of diodes D_2 and D_3 are as follows:

$M_{D2}= \frac{VD2}{VOUT}=\frac{1}{2-D+(1-D)N2+N3}$ (10)

$M_{D3}= \frac{VD4}{VOUT}=\frac{n3}{2-D+(1-D)N2+N3}$ (11)

Equations (7)–(11) illustrate the maximum voltage stress on each power devices.

4. Simulation Results

The Passive Lossless Clamped (PLC) Converter with three-winding coupled output inductor is Simulated in both open and closed loop system using MATLAB simulink and the results are presented. Scope is connected to display the output voltage.

The following values are found to be a near optimum for the design specifications:

Table 4.1 Simulation Parameters

Parameter	Rating
Input voltage	30V
Magnetizing inductor L_m	94µH
$C_1= C_2= C_3$	220µF

L	1 µH
C	1000 µF
$L_{k1}=L_{k2}=L_{k3}$	500 µH
Switching Frequency	50kHz
Diode	IN 4007
MOSFET	IRF840
Turns ratio (coupled inductor set)	1:1:1.5
R	200Ω

4.1 Open Loop Sysem

4.1.1 Conventional Boost Converter

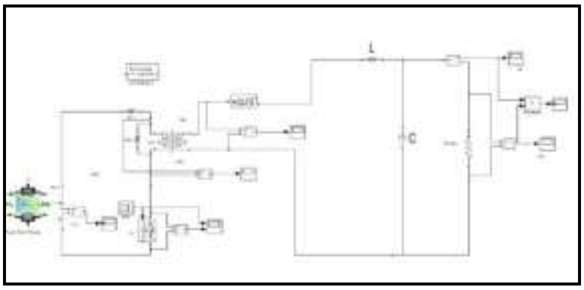

Figure.4.1 Simulated diagram of Conventional boost converter

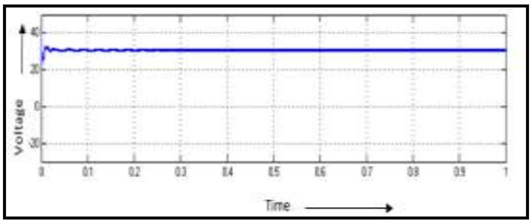

Figure.4.2 Input Voltage

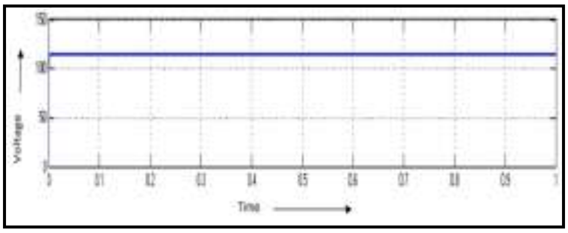

Figure.4.3 Output Voltage

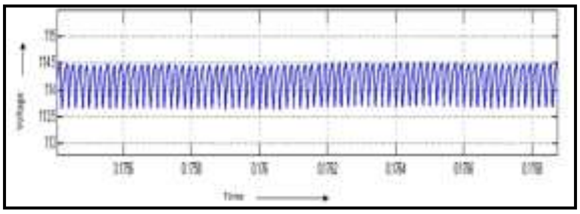

Figure.4.4 Ripple Voltage

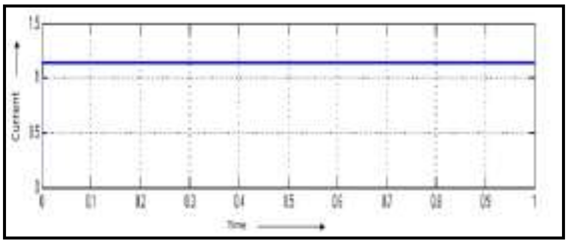

Figure.4.5 Output Current

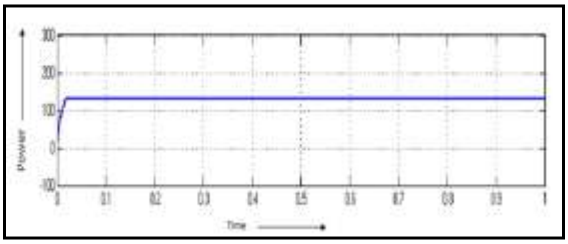

Figure.4.6 Output Power

4.1.2 Passive Lossless Clamped (PLC) Converter with LC Filter

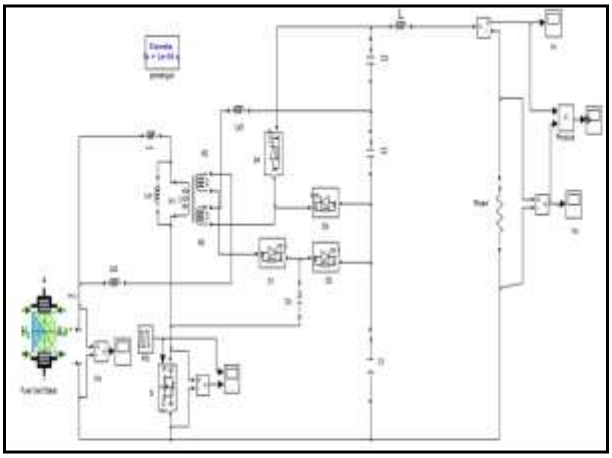

Figure.4.7 Simulated diagram of Passive Lossless Clamped (PLC) Converter with LC Filter

4.1.3 Passive Lossless Clamped (PLC) Converter with Pi Filter

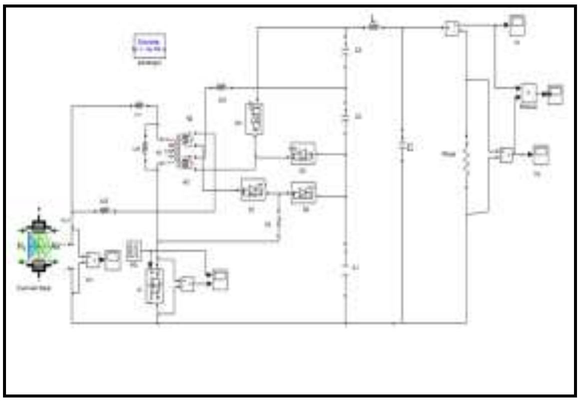

Figure.4.8 Simulated diagram of Passive Lossless Clamped (PLC) Converter with Pi Filter.

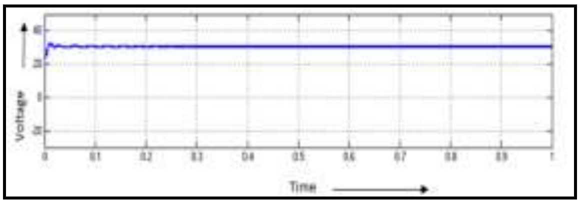

Figure.4.9 Input voltage

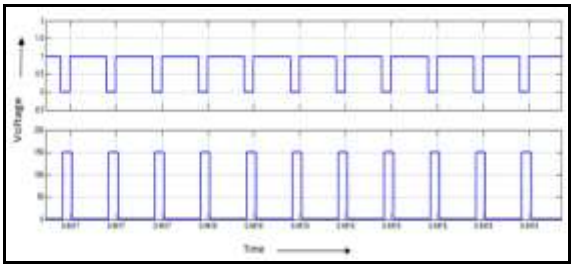

Figure.4.10 Switching pulse M1 &Vds

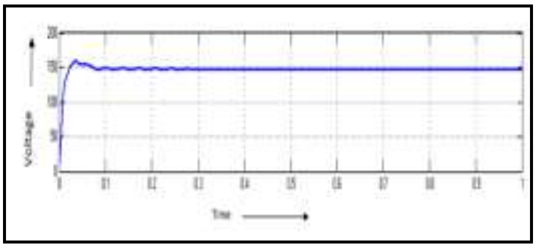

Figure.4.11 Output voltage

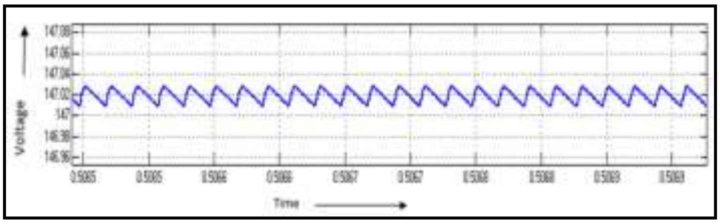

Figure.4.12 Output ripple voltage

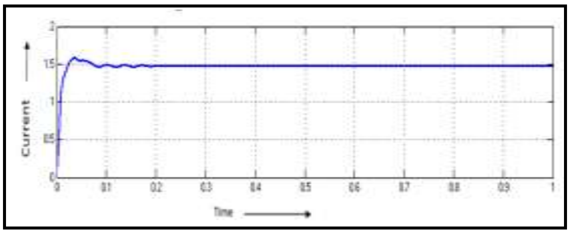

Figure.4.13 Output current

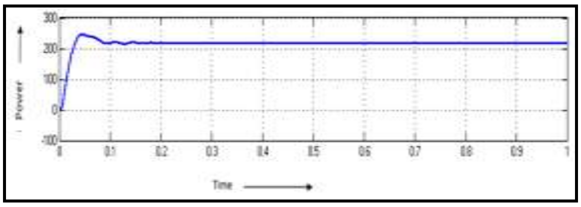

Figure.4.14 Output power

4.1.4 Passive Lossless Clamped (PLC) Converter with Motor Load

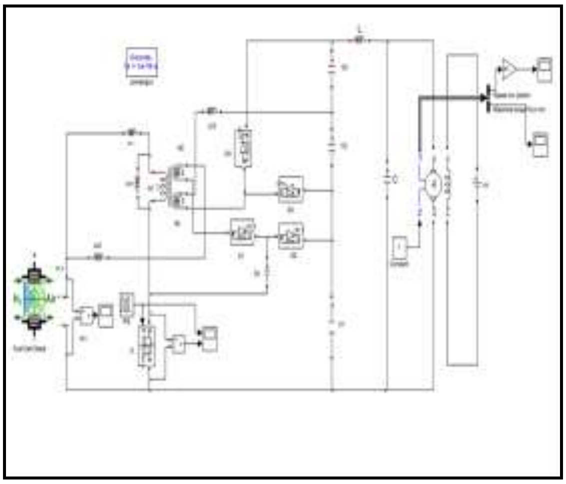

Figure.4.15 Simulated circuit diagram Passive Lossless Clamped (PLC) Converter with Motor Load

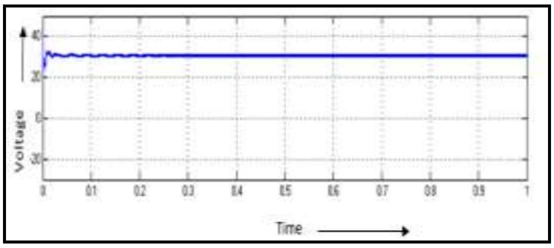

Figure.4.16 Input voltage

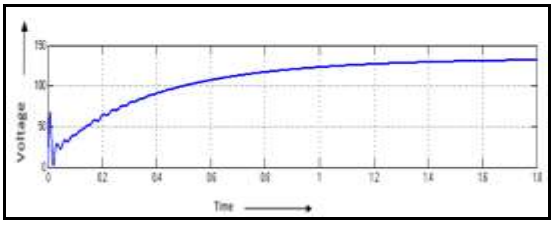

Figure.4.17 Output voltage

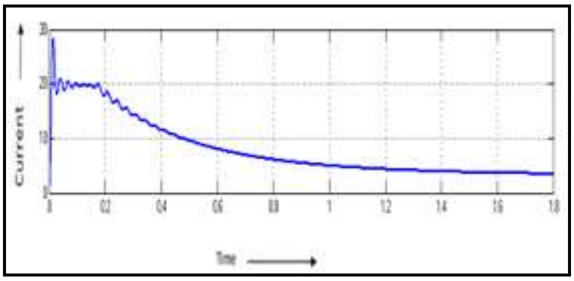

Figure.4.18 Output current

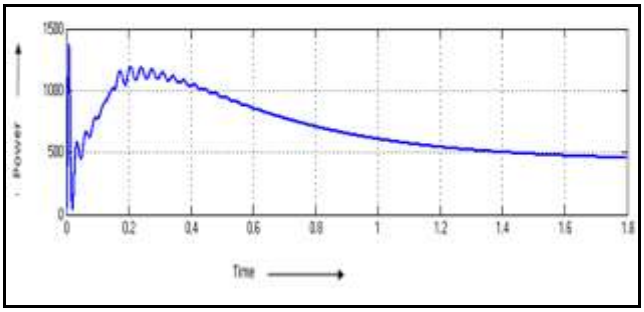

Figure.4.19 Output power

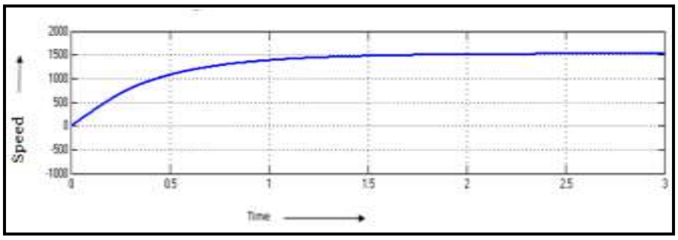

Figure.4.20 Motor speed

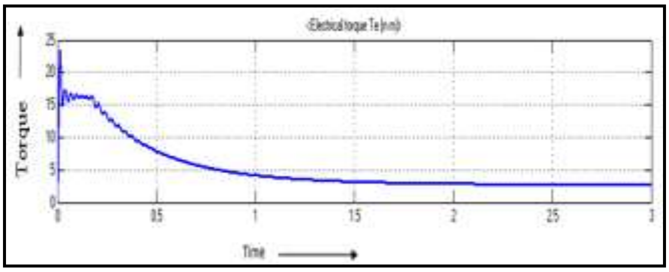

Figure.4.21 Torque

4.1.5 Passive Lossless Clamped (PLC) Converter with Disturbance

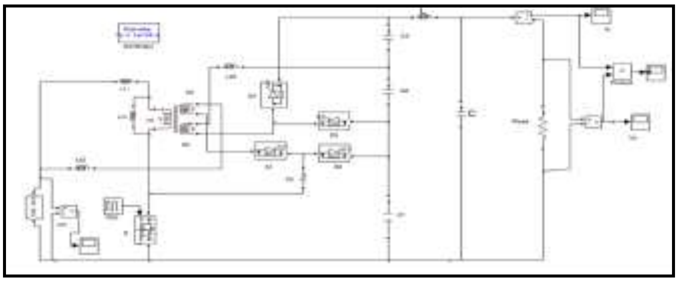

Figure.4.22 Simulated diagram of Passive Lossless Clamped (PLC) Converter with Disturbance

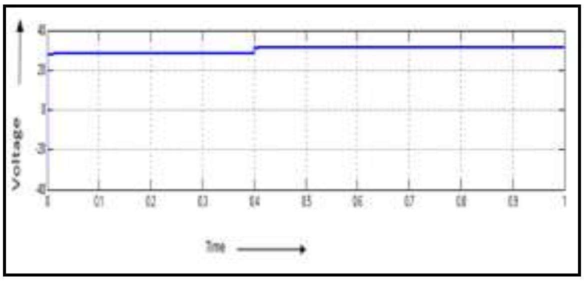

Figure.4.23 Input voltage

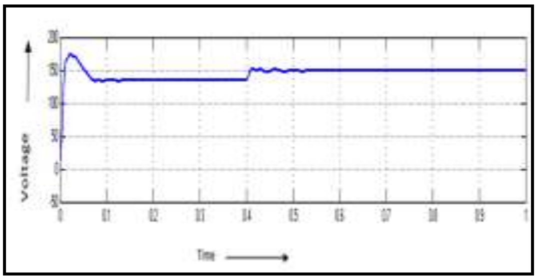

Figure.4.24 Output voltage

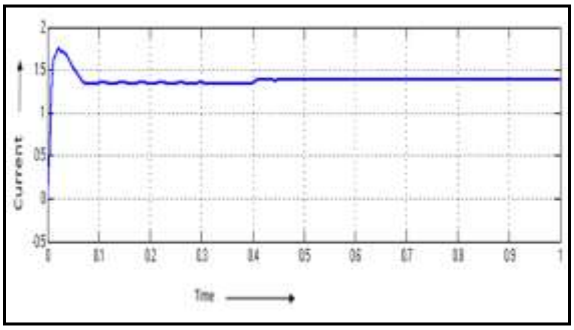

Figure.4.25 Output current

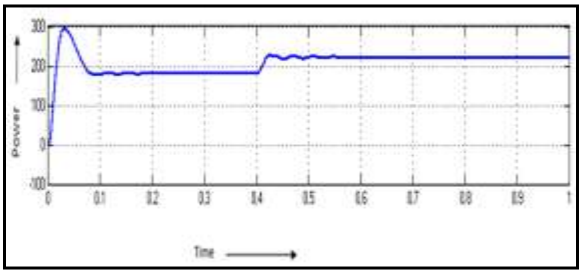

Figure.4.26 Output power

Table 4.2: Comparison between Conventional boost converter and Passive lossless clamped (PLC) Converter

Parameters	Conventional boost Converter	Passive lossless clamped Converter
Input Voltage	35V	35V
Output Voltage	115V	150V
Ripple Voltage	0.5V	0.02V
Output Current	1.1A	1.5A
Output Power	125W	224W

Table 4.3 : Comparison between Passive lossless clamped Converter with LC and PI filter

Parameters	PLC Converter with LC Filter	PLC Converter with Pi Filter
Input Voltage	35V	35V
Output Voltage	150V	150V
Ripple Voltage	0.1V	0.02V
Output Current	1.5A	1.5A
Output Power	224W	224W
Delay Time (t_d)	0.0005s	0.007s
Rise Time (t_r)	0.015s	0.01s
Peak Time (t_p)	0.01s	0.025s
Settling Time (t_s)	0.28s	0.28s

Table 4.4: Comparison between Passive lossless clamped (PLC) converter with Resistive and Motor load

Parameters	PLC Converter with Resistive load	PLC Converter with Motor load
Input Voltage	35V	35V

Output Voltage	150V	130V
Output Current	1.5A	2A
Output Power	224W	500W
Delay Time (t_d)	0.0005s	0.2s
Rise Time (t_r)	0.015s	0.6s
Peak Time (t_p)	0.01s	1.4s
Settling Time (t_s)	0.28s	1.5s

Table 4.5: Comparison between Passive lossless clamped (PLC) converter with and without Disturbance

Parameters	**PLC converter without Disturbance**	**PLC converter with Disturbance**
Input Voltage	35V	35V
Output Voltage	150V	150V
Output Current	1.5A	1.4A
Output Power	224W	220W
Delay Time (t_d)	0.0005s	0.41s
Rise Time (t_r)	0.015s	0.43s
Peak Time (t_p)	0.01s	0.45s
Settling Time (t_s)	0.28s	0.48s

4.2 Closed Loop System

4.2.1 Passive Lossless Clamped (PLC) Converter with PI Controller

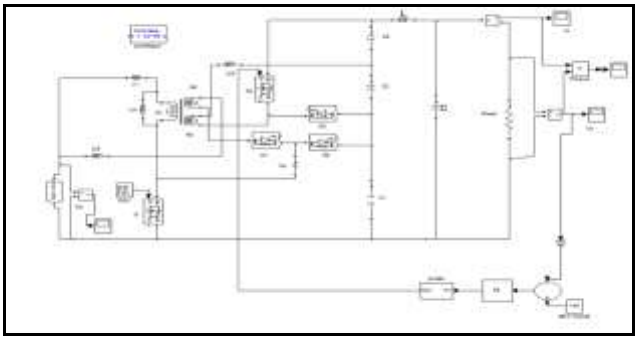

Figure.4.27 Simulated diagram of PLC with PI controller

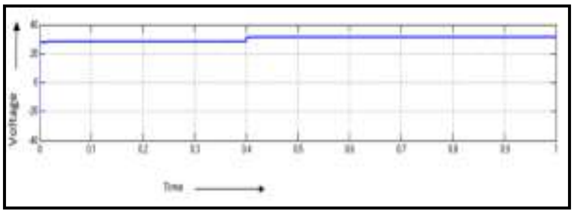

Figure.4.28 Input voltage

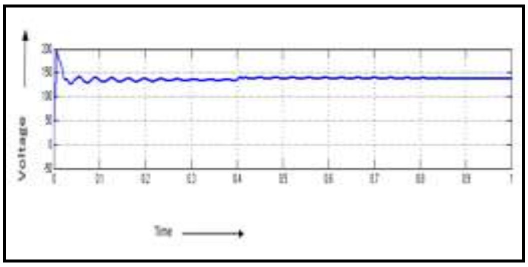

Figure.4.29 Output voltage

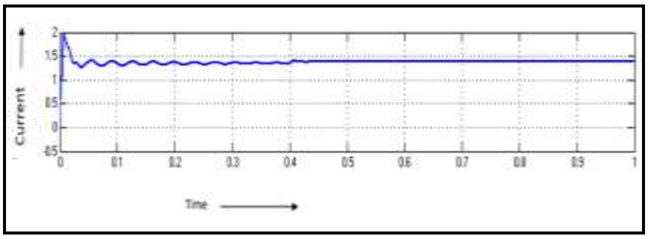

Figure.4.30 Output current

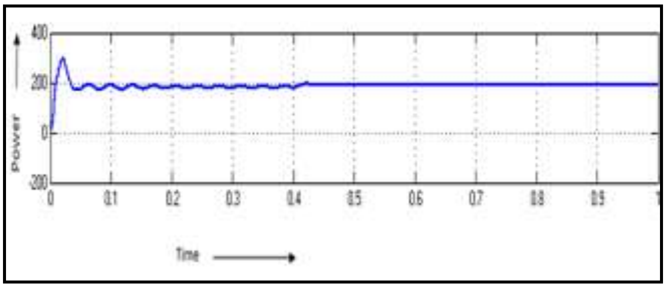

Figure.4.31 Output power

4.2.2 Passive Lossless Clamped (PLC) Converter with PID Controller

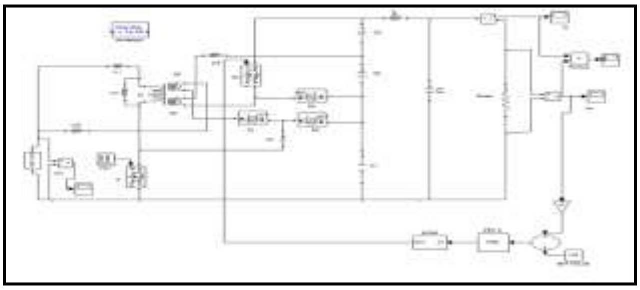

Figure.4.32 Simulated diagram of PLC with PID controller

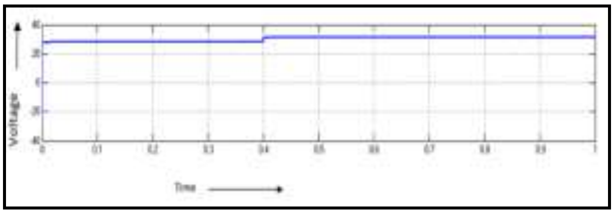

Figure.4.33 Input voltage

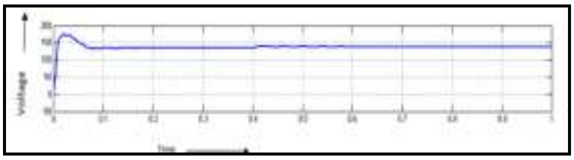

Figure.4.34 Output voltage

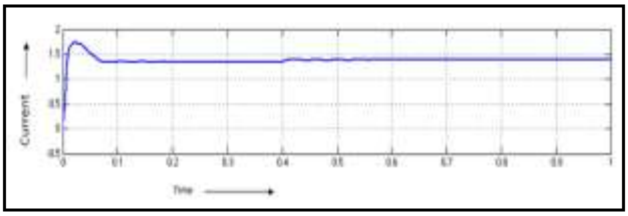

Figure.4.35 Output current

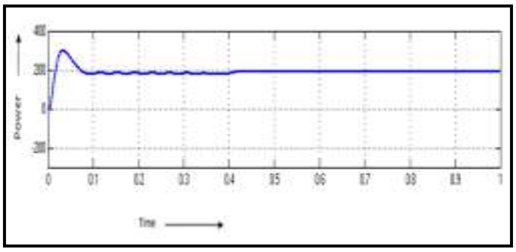

Figure.4.36 Output power

4.2.3 Passive Lossless Clamped (PLC) Converter with Fuzzy Controller

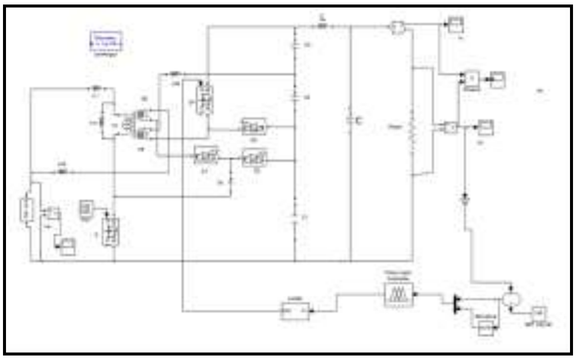

Figure.4.37 Simulated diagram of PLC with FUZZY controller

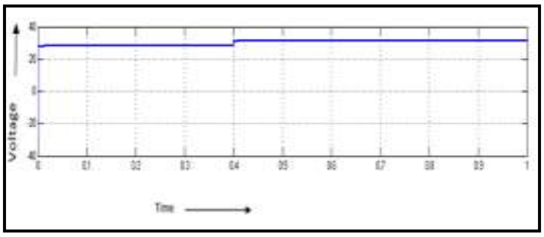

Figure.4.38 Input voltage

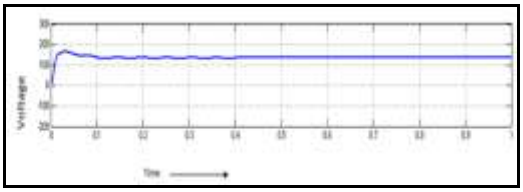

Figure.4.39 Output voltage

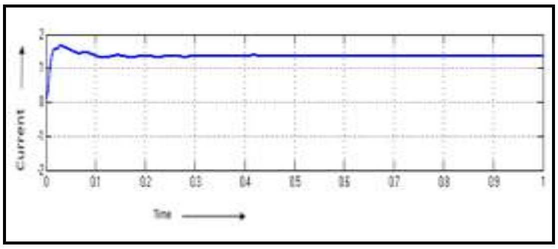

Figure.4.40 Output current

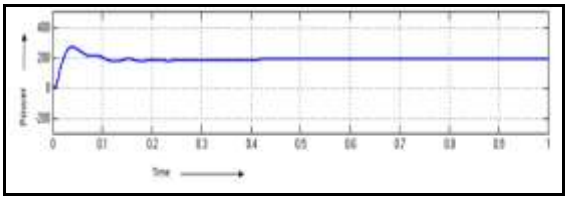

Figure.4.41 Output power

Table 4.6: Comparison of (PLC) Converter with PI,PID,FUZZY Controller

Parameters	PLC with PI Controller	PLC with PID Controller	PLC with FUZZY Controller
Input Voltage	35V	35V	35V
Output Voltage	140V	140V	140V
Output Current	1.4A	1.4A	1.4A
Output Power	200W	200W	200W
Rise Time (t_r)	0.04s	0.03s	0.02s
Peak Time (t_p)	0.47s	0.43s	0
Settling Time (t_s)	0.84s	0.57s	0
Steady state Error(Ess)	1.2	0.9	0.05

5. Hardware Results

Passive Lossless Clamped(PLC) converter is developed and tested in the laboratory. The proposed converter consists of two stages , boosting the voltage generated from the fuel cell through three winding coupled output inductor is done in the first stage and then voltage doubler circuit is used in the second stage. The two stages are driven by a single MOSFET switch. The boost converter consists of three winding coupled output inductor T_r,MOSFET, diodes D_1,D_2,D_3 and D_4 , the switched capacitor C_b , magnetizing inductor and leakage inductors. The voltage doubler circuit consists of output filter capacitors C_1, C_2 and C_3 .

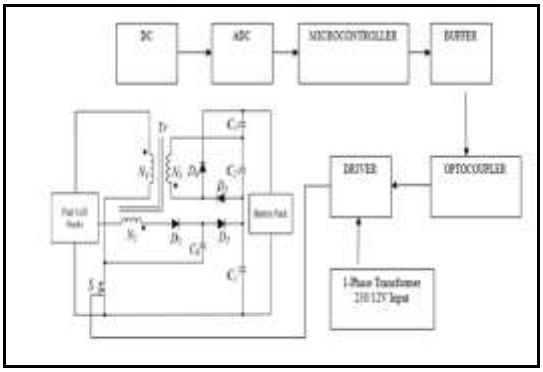

Figure 5.1 Schematic Diagram of Passive Lossless Clamped(PLC) converter

Figure 5.1 shows the schematic diagram of Passive Lossless Clamped(PLC) converter. PLC is the combination of boost converter and voltage doubler circuit . Pulses required for the MOSFET are generated by using a ATMEL microcontroller 89C2051.These pulses are amplified by using a driver amplifier. The driver amplifier is connected between the optocoupler and MOSFET gate. The gate pulses are given to the MOSFET of the Passive Lossless Clamped(PLC) converter . ADC0808 is used for interfacing analog circuit and comparator circuit. To isolate power circuit and control circuit optocoupler is used.8051 microcontroller has two 16-bit timer/counter registers namely timer 1 and timer 2. Both can be configureured to operate either as timers or event counters in the proposed converter

Table 5.1 Hardware Parameters

Parameter	**Rating**
Input voltage	15V
Magnetizing inductor L_m	170µH
C_1= C_2= C_3	220µF
L	500 µH
C	1000 µF
L_{k1}=L_{k2}= L_{k3}	500 µH
Switching Frequency	50kHz
Diode	IN 4007
MOSFET	IRF840
Turns ratio (coupled inductor set)	1:1:1.5
R	200Ω
Regulator	LM7805,LM7812,5-24V
Driver IC	IR2110,+500V or +600V
Crystal Oscillator	230/15V,500mA,50Hz

Figure.5.2 Experimental setup of Passive Lossless Clamped(PLC) converter

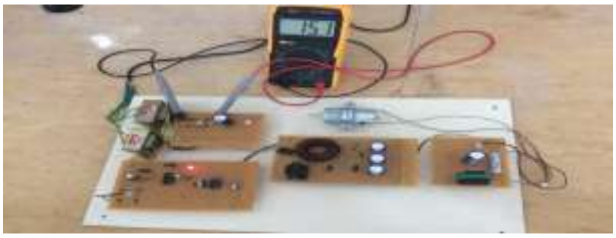

Figure.5.3 Input voltage

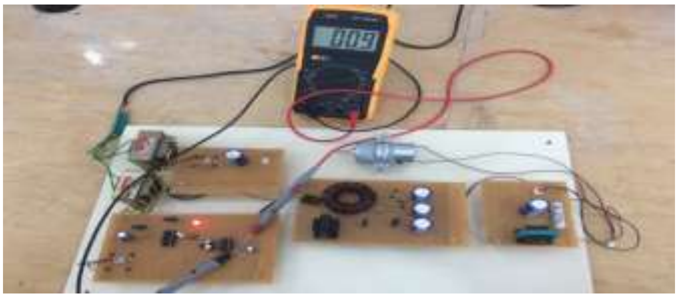

Figure.5.4 Pulse voltage

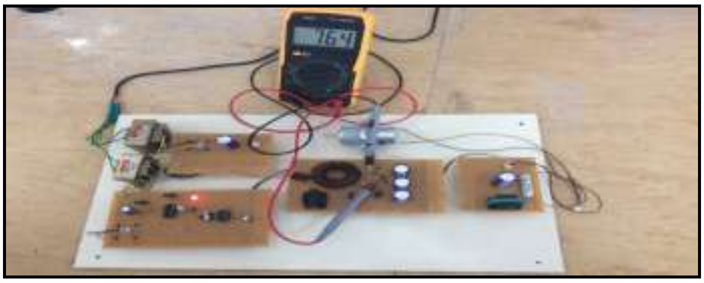

Figure.5.5 Output voltage without Pi filter

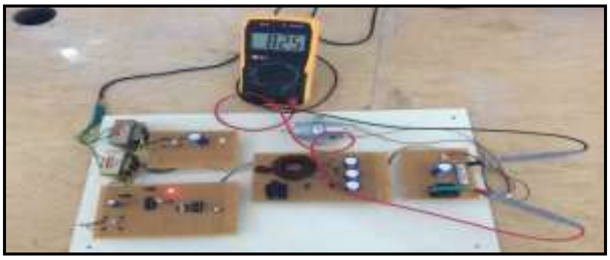

Figure.5.6 Output voltage with Pi filter

Figure.5.7 Gate pulse of MOSFET

Figure.5.8 Drain source voltage

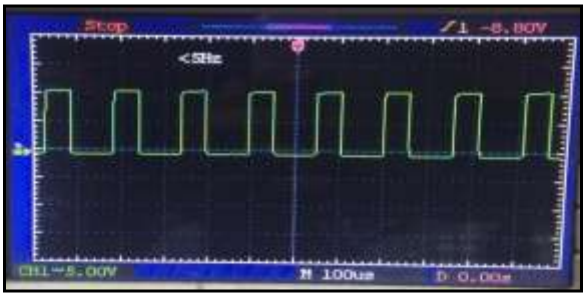

Figure.5.9 Driver output voltage

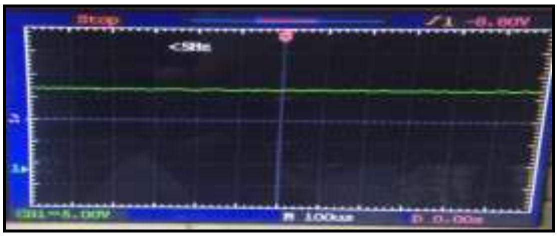

Figure.5.10 DC Input voltage

Figure.5.11 DC output voltage

6. **Conclusion**

In this paper, a passive lossless clamped converter is simulated in open and closed loop by using matlab simulink. By using three-winding coupled output inductor, switched capacitor and voltage doubler circuit, the proposed converter achieves high step-up voltage gain without large duty cycle. By using switched-capacitor, the proposed converter reduces the conduction losses, the voltage stress on the main switch is clamped to a maximum voltage. From open loop system the passive lossless clamped converter with Pi filter gives the better output with less ripple voltage. In closed loop system the comparison is done by using PI,PID and FUZZY controller. The Fuzzy controller results in negligible Rise time, Peak time,Settling time and Delay time .The steady state error is also less by using FUZZY controller.The performance of the proposed converter with FUZZY controller is found better instead of PID Controller.

Finally, the fuel cell as input voltage source is integrated into a prototype converter was implemented and successfully verified. The advantages of the proposed converter are small size and high conversion efficiency, make them valuable and potential. Thus, the passive lossless clamped converter is suitable for high-power application such as fuel cell Hybrid Electric Vehicle.

References

1. Dwari.S.M and Parsa.L, "A novel high efficiency high power interleaved coupled-inductor boost DC–DC converter for hybrid and fuel cell electric vehicle," in *Proc. IEEE Veh. Power Propulsion Conf.*, Sep. 2007, pp. 399–404.
2. Erickson.R.W and Maksimovic,.D, *Fundamentals of Power Electronics*, 2nd ed. New York, NY, USA: Springer, 2001.
3. FinneyS.J, WilliamsB.W, and T. C. Green, "RCD snubber revisited," *IEEE Trans. Ind. Appl.*, vol. 32, no. 1, pp. 155–160, Jan./Feb 1996.
4. Hegazy.O, Van Mierlo.J, and Lataire.P, "Analysis, modeling, and implementation of a multidevice interleaved dc/dc converter for fuel cell hybrid electric vehicles," *IEEE Trans. Power Electron.*, vol. 27, no. 11, pp. 4445–4458, Nov. 2012.
5. Jiang.W and Fahimi.B, "Active current sharing and source management in fuel cell-battery hybrid power system," *IEEE Trans. Ind. Electron.*, vol. 57, no. 2, pp. 752–761, Feb. 2010.
6. Samuel Rajesh Babu R., Deepa S.and Jothivel S., " A comparative analysis of Integrated Boost Flyback converter using PID and Fuzzy controller ", **IJPEDS** ,Volume 5,no 4, April 2015, pp-486-501.
7. Khaligh.A and Li.Z, "Battery, ultracapacitor, fuel cell, and hybrid energy storage systems for electric, hybrid electric, fuel cell, and plug-in energy source applications: State of the art," *IEEE Trans. Veh. Technol.*, vol. 59, no. 6, pp. 2806–2814, Jul. 2010
8. KsiazekP.Z andOrdonez,.M "Swinging bus technique for ripple current elimination in fuel cell power conversion," *IEEE Trans. Power Electron*, vol. 29, no. 1, pp. 170–178, Jan. 2014.
9. Li.W, Lv, Y. Deng.X, Liu.J, and He.X, "A review of non-isolated high step-up DC/DC converters in renewable energy applications," in *Proc.IEEE Appl. Power Electron. Conf. Expo.*, Feb. 2009, pp. 364–369.
10. Li.W and He.X, "Review of nonisolated high-step-up DC/DC converters in photovoltaic grid-connected applications," *IEEE Trans. Ind. Electron.*, vol. 58, no. 4, pp. 1239–1250, Apr. 2011.
11. Laughton.M.A, "Fuel cells," *IEE Eng. Sci. Edu. J.*, vol. 11, no. 1, pp. 7– 16, Feb. 2002.
12. Marchesoni.M and Vacca.C, "New DC–DC converter for energy storage system interfacing in fuel cell energy source applications," *IEEE Trans.Power. Electron.*, vol. 22, no. 1, pp. 301–308, Jan. 2007.
13. Pressman,A.I .Billings.K, and Morey.T, *Switching Power SupplyDesign*, 3rd ed. New York, NY, USA: McGraw-Hill, 2009.
14. Samuel Rajesh Babu R., Deepa S.and Jothivel S., " A Closed loop control of Quadratic boost converter using PID controller ", IJE TRANSACTIONS B: Applications, Vol. 27, No. 11 (November 2014) 1653-1662.
15. PrasannaU.R, Xuewei,P,Rathore.A.K and Rajashekara.K, "Propulsion system architecture and power conditioning topologies for fuel cell vehicles," in *Proc. IEEE Energy Convers. Congr. Expo.*, pp. 1385–1392
16. Rathore.A.K and Prasanna.U.R, "Analysis, design, and experimental results of novel snubberless bidirectional naturally clamped ZCS/ZVS current-fed half-bridge dc/dc converter for fuel cell vehicles," *IEEE Trans.Ind. Electron.*, vol. 60, no. 10, pp. 4482–4491, Oct. 2013

17. Serine.M, Saito.A, and Matsuo.H, "High efficiency DC/DC converter circuit using charge storage diode snubber," in *Proc. 29th Int. Telecommun. Energy Conf.*, 2007, pp. 355–361.

*****